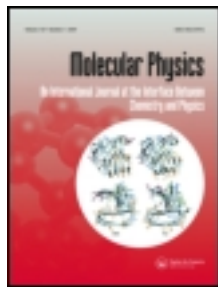


This article was downloaded by: [Aston University]

On: 20 January 2014, At: 16:44

Publisher: Taylor & Francis

Informa Ltd Registered in England and Wales Registered Number: 1072954 Registered office: Mortimer House, 37-41 Mortimer Street, London W1T 3JH, UK



Molecular Physics: An International Journal at the Interface Between Chemistry and Physics

Publication details, including instructions for authors and subscription information:
<http://www.tandfonline.com/loi/tmph20>

Investigating Excited Electronic States using the Algebraic Diagrammatic Construction (ADC) Approach of the Polarisation Propagator

Michael Wormit^a, Dirk R. Rehn^a, Philipp H. P. Harbach^a, Jan Wenzel^a, Caroline M. Krauter^b, Evgeny Epifanovsky^c & Andreas Dreuw^a

^a Interdisciplinary Center for Scientific Computing, University of Heidelberg, Germany

^b Institute of Physical Chemistry, University of Heidelberg, Germany

^c Department of Chemistry, University of California, Berkeley, California 94720, US

Accepted author version posted online: 28 Oct 2013. Published online: 28 Oct 2013.

To cite this article: Molecular Physics (2013): Investigating Excited Electronic States using the Algebraic Diagrammatic Construction (ADC) Approach of the Polarisation Propagator, Molecular Physics: An International Journal at the Interface Between Chemistry and Physics, DOI: [10.1080/00268976.2013.859313](https://doi.org/10.1080/00268976.2013.859313)

To link to this article: <http://dx.doi.org/10.1080/00268976.2013.859313>

Disclaimer: This is a version of an unedited manuscript that has been accepted for publication. As a service to authors and researchers we are providing this version of the accepted manuscript (AM). Copyediting, typesetting, and review of the resulting proof will be undertaken on this manuscript before final publication of the Version of Record (VoR). During production and pre-press, errors may be discovered which could affect the content, and all legal disclaimers that apply to the journal relate to this version also.

PLEASE SCROLL DOWN FOR ARTICLE

Taylor & Francis makes every effort to ensure the accuracy of all the information (the "Content") contained in the publications on our platform. However, Taylor & Francis, our agents, and our licensors make no representations or warranties whatsoever as to the accuracy, completeness, or suitability for any purpose of the Content. Any opinions and views expressed in this publication are the opinions and views of the authors, and are not the views of or endorsed by Taylor & Francis. The accuracy of the Content should not be relied upon and should be independently verified with primary sources of information. Taylor and Francis shall not be liable for any losses, actions, claims, proceedings, demands, costs, expenses, damages, and other liabilities whatsoever or howsoever caused arising directly or indirectly in connection with, in relation to or arising out of the use of the Content.

This article may be used for research, teaching, and private study purposes. Any substantial or systematic reproduction, redistribution, reselling, loan, sub-licensing, systematic supply, or distribution in any form to anyone is expressly forbidden. Terms & Conditions of access and use can be found at <http://www.tandfonline.com/page/terms-and-conditions>

RESEARCH ARTICLE

Investigating Excited Electronic States using the Algebraic Diagrammatic Construction (ADC) Approach of the Polarisation Propagator

Michael Wormit^{*,a}, Dirk R. Rehn^a, Philipp H. P. Harbach^a, Jan Wenzel^a, Caroline M. Krauter^b, Evgeny Epifanovsky^c, and Andreas Dreuw^a

^a *Interdisciplinary Center for Scientific Computing, University of Heidelberg, Germany*

^b *Institute of Physical Chemistry, University of Heidelberg, Germany*

^c *Department of Chemistry, University of California, Berkeley, California 94720, US*

(Received 00 Month 200x; final version received 00 Month 200x)

The development of reliable theoretical methods and the provision of efficient computer programs for the investigation of optical spectra and photochemistry of large molecules in general is one of the most important tasks of contemporary theoretical chemistry. Here, we present an overview of the current features of our implementation of the algebraic diagrammatic construction (ADC) scheme of the polarisation propagator, which is a versatile and robust approach for the theoretical investigation of excited states and their properties.

Keywords: algebraic diagrammatic construction; polarisation propagator; excited states;

1. Introduction

The theoretical investigation of the photochemistry of medium-sized and large molecules with more than say 20 atoms of the second row of the periodic table is one of the most challenging tasks of contemporary quantum chemistry [1–6]. This reaches from the accurate description of optical spectra, all the way to the identification and investigation of photo-initiated processes like for example excited state proton transfer, photo-induced electron transfer, photo-isomerization, or photo-dissociation. A detailed understanding of such photoreactions requires knowledge of the potential energy surfaces of the involved excited states along relevant reaction coordinates, since shape and the topologies of the PES, most importantly conical intersections, determine the photochemistry of molecules [7].

At present, linear-response time-dependent density functional theory (TDDFT) [8–10] is by far the most widely used method for the investigation of excited state properties and photochemistry of large molecules (see for example [3, 11–13]). This owes to its low computational demands and its documented accuracy for local valence state energetically well below the ionization potential [10, 14]. However, TDDFT is also known to exhibit drastic failures for charge-transfer excited states and doubly excited states when standard exchange-correlation (xc) functionals are employed [15–17]. These failures are recently addressed by including wavefunction-based components in the xc-functionals via long-range non-local orbital exchange in

*Corresponding author. Email: michael.wormit@iwr.uni-heidelberg.de

so-called LRS functionals [18–24] or second-order schemes for electron correlations or doubly excited states in double hybrid functionals [25, 26]. These manipulations of the xc functional have strong semi-empirical character and take away the original gist of DFT demanding the xc potential to be a local in space [27]. In addition, when second-order wavefunction schemes are included in the xc functional, the computational cost of a TDDFT calculation increases drastically [25, 26]. Owing to the approximate character of the xc functionals, thorough comparison with experiment or higher level computations is required as benchmark to ensure correctness of the TDDFT calculations [2]. These benchmarks can nowadays be provided by powerful wavefunction-based methods like complete active-space self-consistent field (CASSCF) methods [28, 29], symmetry-adapted cluster configuration interaction (SAC-CI) [30] and also approximate linear-response coupled-cluster theory of second order (RI-CC2) [31, 31–34]. In recent years also polarisation-propagator based approaches like SOPPA and ADC(2) received increasing attention [17, 35–40].

To get into the position to study photochemistry of large molecules reliably, it is thus important to increase the range of applicability of wavefunction-based methods. In this paper, we aim at presenting theoretical and computational aspects of the algebraic diagrammatic construction (ADC) scheme of the polarisation propagator for the calculation of excited electronic states and their properties. To be self-contained, the basic principles of its derivation via the intermediate state representation will be outlined, and several levels of approximation will be introduced. The ease of implementing ADC-based methods within our `adcm` module of Q-Chem is highlighted. For the first time, a newly developed, very efficient implementation of core-valence-separated ADC methods is presented and first preliminary results are shown which demonstrate its accuracy. Another focus is put on the presentation of how excited state and transition properties are calculated exploiting the one-particle transition density matrix and the one-particle reduced density matrices of the excited states and of transitions between excited states. These matrices can further be visualized to analyze the electronic structure of the excited states and the character of electronic transitions.

2. Theory

The ADC scheme for the calculation of excited electronic states has been originally derived in the context of diagrammatic many-body propagator theory [38]. In this context electronic excitations of a system are described by the polarisation propagator whose spectral representation is given by

$$\Pi_{pq,rs}(\omega) = \sum_{n \neq 0} \left[\frac{\langle \Psi_0 | \hat{c}_p^\dagger \hat{c}_q | \Psi_n \rangle \langle \Psi_n | \hat{c}_r^\dagger \hat{c}_s | \Psi_0 \rangle}{\omega - (E_n - E_0) + i\eta} - \frac{\langle \Psi_0 | \hat{c}_r^\dagger \hat{c}_s | \Psi_n \rangle \langle \Psi_n | \hat{c}_p^\dagger \hat{c}_q | \Psi_0 \rangle}{\omega + (E_n - E_0) - i\eta} \right] \quad (1)$$

Here $|\Psi_0\rangle$, $|\Psi_n\rangle$ are the ground and excited states of the N-electron system with energies E_0 and E_n , respectively. The operators \hat{c}_p^\dagger and \hat{c}_q are the usual creation and annihilation operators of single-particle wavefunctions φ_p , often chosen to be the Hartree-Fock orbitals. The complex term $i\eta$ in the denominators originates from a Fourier transform necessary to arrive at the spectral representation. By taking the limit $\eta \rightarrow 0$ this term vanishes and will subsequently be omitted.

Examining the structure of the polarisation propagator it becomes apparent that it possesses poles at the positive and negative vertical excitation energies, while the respective residues provide a measure for the probability of the transition from the ground to the excited state.

The ADC scheme reformulates the spectral representation of the polarisation propagator by recognising eq. (1) as the "diagonal" representation

$$\Pi_{pq,rs}(\omega) = \mathbf{x}_{pq}^\dagger (\omega \mathbf{1} - \mathbf{\Omega})^{-1} \mathbf{x}_{rs} - \mathbf{x}_{rs}^\dagger (\omega \mathbf{1} + \mathbf{\Omega})^{-1} \mathbf{x}_{pq} \quad (2)$$

of a more general bilinear form. Here, $\mathbf{\Omega}$ refers to the diagonal matrix of excitation energies with matrix elements $\Omega_{n,m} = (E_n - E_0) \delta_{nm}$, while \mathbf{x}_{pq} is the vector of "spectroscopic" amplitudes with elements $x_{pq,n} = \langle \Psi_n | \hat{c}_p^\dagger \hat{c}_q | \Psi_0 \rangle$. Thus, instead of using the "basis" of exact N-electron excited states the polarisation propagator can also be expressed in terms of a different orthogonal basis of intermediate state (IS) $|\tilde{\psi}_I\rangle$ spanning the same space of N-electron functions. As result, the intermediate state representation (ISR) of the polarisation propagator is obtained as

$$\Pi_{pq,rs}(\omega) = \mathbf{f}_{pq}^\dagger (\omega \mathbf{1} - \mathbf{M})^{-1} \mathbf{f}_{rs} - \mathbf{f}_{rs}^\dagger (\omega \mathbf{1} + \mathbf{M})^{-1} \mathbf{f}_{pq} \quad (3)$$

where $M_{IJ} = \langle \tilde{\psi}_I | \hat{H} - E_0 | \tilde{\psi}_J \rangle$ and $f_{pq,I} = \langle \tilde{\psi}_I | \hat{c}_p^\dagger \hat{c}_q | \Psi_0 \rangle$ are the shifted Hamiltonian matrix and the "spectroscopic" amplitudes in the IS basis, respectively. In the preceding equations the polarisation propagator has been expressed as a sum of two terms each of which contain the same physical information. Thus, the second term can in principle be omitted.

To explicitly construct the IS basis the ADC scheme starts from the Møller-Plesset perturbation expansion of the ground state and applies excitation operators to it, before orthogonalizing the resulting set of states [41, 42]. Thereby, a perturbation expansion of the IS basis is obtained from which perturbation series of the Hamiltonian matrix

$$\mathbf{M} = \mathbf{M}^{(0)} + \mathbf{M}^{(1)} + \mathbf{M}^{(2)} + \dots \quad (4)$$

and the spectral amplitudes

$$\mathbf{f}_{pq} = \mathbf{f}_{pq}^{(0)} + \mathbf{f}_{pq}^{(1)} + \mathbf{f}_{pq}^{(2)} + \dots \quad (5)$$

can be derived so that the polarisation propagator is expressed consistently to a certain order. The emerging structure of \mathbf{M} and \mathbf{f}_{pq} is displayed in Figure 1. Explicit equations for \mathbf{M} up to third order in perturbation theory can be found elsewhere [43]. From them the excited states are obtained by diagonalization of the hermitian matrix \mathbf{M}

$$\mathbf{M}\mathbf{Y} = \mathbf{Y}\mathbf{\Omega} \quad \mathbf{Y}^\dagger \mathbf{Y} = \mathbf{1} \quad (6)$$

yielding the excitation energies $\Omega_n = E_n - E_0$ as eigenvalues. The eigenvectors \mathbf{Y}_n provide access to the excited state wave functions via the relation

$$|\psi_n\rangle = \sum_J |\tilde{\psi}_J\rangle Y_{n,J} \quad (7)$$

and to the one-particle reduced transition density matrices by combining the ISR of the spectroscopic amplitude vectors \mathbf{f}_{pq} and the eigenvectors \mathbf{Y}

$$\rho_{pq}^{n\leftarrow 0} = \langle \Psi_n | c_p^\dagger c_q | \Psi_0 \rangle = \sum_I Y_{n,I}^\dagger \langle \tilde{\psi}_I | c_p^\dagger c_q | \Psi_0 \rangle = \mathbf{Y}_n^\dagger \mathbf{f}_{pq} \quad (8)$$

Furthermore, the eigenvectors can be used to compute the one-particle reduced density matrices of the excited states and the one-particle reduced transition density matrices for transitions between excited states via

$$\rho_{pq}^{m \leftarrow n} = \langle \psi_m | c_p^\dagger c_q | \psi_n \rangle = \sum_{I,J} Y_{m,I}^\dagger \langle \tilde{\psi}_I | c_p^\dagger c_q | \tilde{\psi}_J \rangle Y_{n,J} = \mathbf{Y}_m^\dagger \mathbf{B}_{pq} \mathbf{Y}_n \quad (9)$$

where \mathbf{B}_{pq} is the matrix of IS transition densities. The excited state density matrix results from the above equation by setting $n = m$, i.e. $\rho_{pq}^n = \rho_{pq}^{n \leftarrow n}$.

With the density and transition density matrices at hand any excited state property T_n or transition property $T_{n \leftarrow 0}$ or $T_{n \leftarrow m}$ which can be expressed in terms of a one-particle operator $\hat{O} = \sum_{pq} O_{pq} \hat{c}_p^\dagger \hat{c}_q$ is now accessible as

$$T_n = \langle \Psi_n | \hat{O} | \Psi_n \rangle = \sum_{pq} O_{pq} \rho_{pq}^n \quad (10)$$

$$T_{n \leftarrow 0} = \langle \Psi_n | \hat{O} | \Psi_0 \rangle = \sum_{pq} O_{pq} \rho_{pq}^{n \leftarrow 0} \quad (11)$$

$$T_{n \leftarrow m} = \langle \Psi_n | \hat{O} | \Psi_m \rangle = \sum_{pq} O_{pq} \rho_{pq}^{n \leftarrow m} \quad (12)$$

In particular, dipole transition moments and oscillator strengths can be computed using the above relations.

A more complex property which can be calculated using the ADC/ISR formalism is the two-photon transition strength δ_{TP}^m for a transition from the ground state to an excited state m . In case of resonant absorption of two linearly polarised photons with the same energy, δ_{TP}^m is given by [44]

$$\delta_{TP}^m = \frac{1}{15} \sum_{\mu, \nu = x, y, z} (S_{\mu\mu}^m S_{\nu\nu}^{m*} + S_{\mu\nu}^m S_{\nu\mu}^{m*} + S_{\mu\nu}^m S_{\nu\mu}^{m*}) \quad (13)$$

where $S_{\mu\nu}^m$ refers to the respective two-photon transition moment which can be expressed as a sum-over-states [45]

$$S_{\mu\nu}^m = \sum_{n \neq 0} \frac{\langle \Psi_0 | \hat{D}'_\mu | \Psi_n \rangle \langle \Psi_n | \hat{D}'_\nu | \Psi_m \rangle + \langle \Psi_0 | \hat{D}'_\nu | \Psi_n \rangle \langle \Psi_n | \hat{D}'_\mu | \Psi_m \rangle}{\Omega_n - \frac{1}{2}\Omega_m} \quad (14)$$

Here, \hat{D}'_μ denotes the cartesian components $\mu = x, y, z$ of the shifted dipole operator $\hat{D}'_\mu = \hat{D}_\mu - \langle \Psi_0 | \hat{D}_\mu | \Psi_0 \rangle$.

By truncating the sum over $n \neq 0$ this expression can be directly evaluated using previously calculated excitation energies and transition dipole moments. However, to obtain a reasonably good approximation of $S_{\mu\nu}^m$ a large number of excited states has to be included which is not always feasible. Instead the ISR formalism can be used to transform eq. (14) into

$$S_{\mu\nu}^m = \mathbf{F}^\dagger(\hat{D}'_\mu) \left[\mathbf{M} - \frac{\Omega_m}{2} \mathbf{1} \right]^{-1} \mathbf{B}(\hat{D}'_\nu) \mathbf{Y}_m + \mathbf{F}^\dagger(\hat{D}'_\nu) \left[\mathbf{M} - \frac{\Omega_m}{2} \mathbf{1} \right]^{-1} \mathbf{B}(\hat{D}'_\mu) \mathbf{Y}_m \quad (15)$$

with the newly introduced quantities $\mathbf{F}(\hat{D}'_\mu)$ and $\mathbf{B}(\hat{D}'_\mu)$ being related to the IS

transition densities via

$$\mathbf{F}(\hat{D}'_{\mu}) = \sum_{pq} D_{pq}^{\mu} \mathbf{f}_{pq} \quad \text{and} \quad \mathbf{B}(\hat{D}'_{\mu}) = \sum_{pq} D_{pq}^{\mu} \mathbf{B}_{pq} - \langle \Psi_0 | \hat{D}_{\mu} | \Psi_0 \rangle \mathbf{1}$$

and D_{pq}^{μ} denoting the matrix elements of the dipole operator \hat{D}_{μ} in terms of the one-particle basis functions.

Equation (15) does no longer involve a sum over the excited states, but can be evaluated by operations on matrix quantities, in particular by using numerical matrix inversion techniques.

3. Overview of Implementation and Features

The suite of ADC methods for electronically excited states (`adcmn`) is available as part of the quantum chemistry package Q-Chem [46, 47]. It features various methods for the calculation of excited states up to third order in perturbation theory, as well as the ability to compute excited state properties and transition properties like two-photon absorption cross sections. Below an overview of the implementation and the capabilities is given including examples of applications.

3.1. Implementation using the Tensor Library

The `adcmn` suite has been implemented as an independent module in Q-Chem with a minimal interface to the rest of the quantum chemical package. This modular design allows for the possibility to combine it with other quantum chemistry packages in future by replacing the interface.

To perform the tensor operations which are required by most wavefunction-based electronic structure methods `adcmn` uses the newly developed general-purpose tensor library `libtensor` [48] in Q-Chem. The tensor library is a C++ template library which is also available as open source. It provides the infrastructure for `adcmn` to create tensors of arbitrary rank and size and perform linear algebra operations on them. The data model which `libtensor` employs divides every tensor into smaller blocks of the same rank by splitting every dimension into several parts. This allows for immediate parallelisation of tensor operations in a shared memory environment, since operations on individual blocks can be performed independently. Furthermore, blocks can be moved separately in and out of memory by the virtual memory management module operating in the background of `libtensor`, if the available memory is not sufficient to accommodate all tensor data.

The library also fully supports symmetry, in particular spin and point group symmetry. Thereby, no special symmetry-adapted versions of the ADC equations are required to perform symmetry-aware calculations. Only the initial tensors at the beginning of an ADC calculation have to be set up appropriately to enable the symmetry adaptation.

For the implementation of the ADC equations an easy-to-use interface is provided by `libtensor` which allows for the direct translation of equations into code, in a similar fashion as they would be written in L^AT_EX. To illustrate this, a part of the equations required for the ADC(2) method is compared to the respective code in Figure 2.

3.2. Calculation of Valence Excited States

For the calculation of energetically low-lying excited states the ADC methods ADC(1), ADC(2), ADC(2)-x and ADC(3) [38, 43] are currently available within `adcm`. Thereby, excited states can be obtained at different levels of accuracy and at quite different computational costs. The lowest level provided is ADC(1) which is exactly identical to the well-known CIS method [49]. Next in the hierarchy are ADC(2) and ADC(2)-x where the former yields excitation energies comparable in quality to the excited state methods CC2 [33, 50] and CIS(D) [51, 52], while the excitation energies generated by the latter come closer to EOM-CCSD [53–55]. Finally, the ADC(3) method provides results with almost the same accuracy as CC3 [31], but at costs which are an order of magnitude smaller. As example, the excitation energies and oscillator strengths of the two lowest excited states of formaldehyde are shown in Table 1 obtained with different ADC methods and various basis sets.

To compute the excited states `adcm` usually employs the Davidson algorithm [56] to find the N smallest eigenvalues of the respective ADC matrix. In case of ADC(2) an alternative method is available [33] which combines Davidson and DIIS algorithm resulting in reduced computational costs. However, this algorithm might not always converge or it might not converge to the intended states, i.e. missing some energetically lower states. Any ADC calculation can exploit the resolution-of-the-identity (RI) approximation to speed-up the transformation of the two-electron integrals from atomic orbitals to molecular orbitals [33]. The full implementation of the ADC equations in terms of the RI integrals is currently work in progress.

To demonstrate the performance of the ADC implementation Figure 3 shows how the calculation speed increases when run on multiple CPU cores for a number of systems with varying sizes. It can clearly be seen from the figure that for small systems, the parallelisation does not improve calculation times. Only when the calculations become more demanding, they start to benefit from the available cores resulting in an almost optimal speed-up in the case of the ADC(3) calculation of benzene with aug-cc-pVDZ basis set.

On the other hand, when the calculation size increases, also the amount of memory required is raised. Thus, as soon as the available memory is exhausted, the additional data has to be written to disk which can increase the time of the calculations significantly. This can be observed in Figure 4 which shows the increase in run time for an ADC(2) calculation of benzene with aug-cc-pVDZ basis set using 8 cores, if the available memory has been limited artificially. In this case, the speed-up due to the 8 cores is almost countermanded when the required memory is four times larger than the available memory.

3.3. Core Excitations using Core-Valence Separated ADC

The calculation of core-excited electronic states is generally tedious, since most implementations of excited-state methods are designed to compute the energetically lowest energy eigenvalues of the excitation spectrum via an iterative diagonalization scheme of the corresponding Hamiltonian matrix, and core-excited states are located at the high-energy edge of the spectrum. An elegant route to core-excited states is provided by the so-called core-valence separation (CVS) approximation [57]. The idea is very simple and relies on the fact that core orbitals are strongly localized in space and energetically well separated from the valence orbitals. As a consequence the interaction between core-excited states and valence-excited states is negligible and the Hamiltonian separates practically naturally into

the spaces of singly core-excited states and valence excited states [57]. Hence, the ADC matrix needs to be built only in the space of singly core-excited states and diagonalized leading to significant computational savings compared to the conventional ADC approach for valence-excited states. The implementation is straightforward as one only needs to restrict the index of the occupied orbital in the ph configurations to correspond to a core orbital and in the 2p2h configurations one of the occupied indices to represent a core orbital. Owing to its hermiticity, ADC methods are particularly well-suited for the use of the CVS approximation, and it has been demonstrated previously that CVS-ADC(2)-x yields excellent results for core-excited states [58–60].

For testing purposes, we have re-computed the core-excited states of thymine using CVS-ADC(2)-x and the standard 6-311++G** basis set containing two sets of diffuse and polarization functions (Table 2), since previously published CVS-ADC(2)-x and near-edge x-ray absorption fine structure (NEXAFS) data are available for direct comparison [58]. As can be seen in Table 2, the agreement between the calculated CVS-ADC(2)-x results and the experimental values is remarkable, in particular when the larger 6-311++G** basis set is employed. It is important to note that no shifting of the computed excitation energies is necessary to achieve this agreement as is typically needed to correct for the inherent errors in the methods, when more approximate methods and smaller basis sets are employed [61]. Summarizing, the available efficient implementation of CVS-ADC(2)-s and CVS-ADC(2)-x in Q-Chem allows for the computation of core-excited states and oscillator strengths and makes direct comparison with x-ray absorption (XAS) and NEXAFS spectra possible.

3.4. Spin-opposite-scaled ADC variants

A straightforward way to simplify the ADC equations is to neglect the same-spin contributions in the ADC matrix and to scale the opposite-spin contribution with appropriate semi-empirical parameters. This idea stems from the underlying MP2 method, which was recognized to underestimate those contributions to the correlation energy arising from electrons with opposite spin while those from electrons with same spin are overestimated [62]. Introduction of two scaling parameters for these two contributions gave rise to SCS-MP2 providing an improved description of the correlation energy [63, 64]. It was further shown that it is even possible to neglect the same-spin contribution completely and to scale the opposite spin component accordingly [65]. These basic ideas have been adopted also to many excited state methods: CIS(D) [66, 67] as well as to two variants of CIS with quasidegenerate second-order perturbation corrections (CIS(D₀) and CIS(D₁)) [68–70], and also to the ri-CC2 method [71, 72] and strict ri-ADC(2) [72].

Recently, we have shown that the ISR formalism as outlined above can be employed to derive a "rigorous" ISR-SOS-ADC(2) method starting from the SOS-MP2 ground state [73]. This, however, does not result in any computational savings or substantial improvement, since only the t_2 -amplitudes contained in the ph/ph block and inherited from the underlying MP2 method are replaced by the ones from SOS-MP2. Instead, following the previous implementation of SOS-ADC(2)-s in TURBOMOLE [71, 72, 74], an SOS-ADC(2)-s scheme has been implemented which requires scaling of the t_2 -amplitudes of the ph/ph block as well as of the matrix elements of the ph/2p2h and 2p2h/ph coupling blocks (Figure 5) with the coefficients c_{os} and c_c , respectively. While $c_{os}=1.3$ is inherited from SOS-MP2 and is left unchanged, c_c has been fitted against the Thiel benchmark set [75], which yielded an optimal value of 1.17 for singlet excited states with predominant single excita-

tion character [73]. Following this procedure a mean absolute error of only 0.14 eV is achieved for all states of the Thiel benchmark set with a standard deviation of 0.11 eV and a maximum absolute error of 0.52 eV.

Application of the SOS approximation also to ADC(2)-x requires the introduction of yet another scaling factor c_x for the off-diagonal elements in the 2p2h/2p2h block (Figure 5). Fitting this set of parameters against the Thiel benchmark set and DFT/MRCI data revealed that optimal results are obtained for both singly and doubly excited states, when $c_{os}=1.3$, $c_c=1.0$ and $c_x=0.9$ [73]. Using these parameters, a mean absolute error of only 0.17 eV is achieved for singlet states with predominantly single excitation character, and 0.21 eV for states with large double excitation character. Hence, within the SOS-ADC(2)-x scheme it is only necessary to scale down the coupling elements within the 2p2h/2p2h block slightly to result in a balanced description of singly and doubly excited states in excellent agreement with the benchmark set [75].

3.5. Transition Properties and Excited State Properties

As described in section 2 transition properties from the ground state to the excited states can be obtained from the excited state eigenvectors \mathbf{Y}_n and the IS spectroscopic amplitudes \mathbf{f}_{pq} (eq. (8) and (11)). Thus, subsequent to every determination of excitation energies and excited state eigenvalues in `adcmn` the transition dipole moment and the related oscillator strength for every ground-to-excited state transition are calculated in `adcmn` by default. In addition, properties of the excited states, like dipole moment or quadrupole moment, can be requested. They are computed using the IS transition densities \mathbf{B}_{pq} via the relations (9) and (10). Similarly, dipole transition moments and transition probabilities for transitions between the excited states can be obtained upon request. As example, Table 3 shows a collection of excited state properties for the four energetically lowest excited states of pyridine.

The excited state data also allows for the determination of two-photon transition strengths using the sum-over-states expression (14). Alternatively, the two-photon transition strength is also available via equation (15). A comparison of the results for the two-photon transition strength using the two methods can be found in Table 4.

3.6. Visualisation of Densities

The calculation of the ADC excited state properties and transition properties requires the prior determination of density matrices and transition density matrices of the excited states. Since these matrices are available anyways, they can be employed for the visualisation by means of transition densities, difference densities or attachment and detachment densities at no significant extra costs.

If requested, the transition densities

$$\Gamma(\mathbf{r}) = \sum_{pq} \phi_p^*(\mathbf{r}) \phi_q(\mathbf{r}) \rho_{qp}^{m \leftarrow n},$$

difference densities

$$\Delta\rho(\mathbf{r}) = \sum_{pq} \phi_p^*(\mathbf{r}) \phi_q(\mathbf{r}) (\rho_{qp}^n - \rho_{qp}^0)$$

or attachment and detachment densities which derive from the difference densities [76] are evaluated on a user specified grid using the respective density matrices and exported as `cube` files. The latter can then be visualised using one of the standard visualisation tools as shown in Figure 6 for the two energetically lowest states of pyridine.

4. Outlook

We present the implementation of a suite of ADC methods for the reliable calculation of excited states and their properties as well as transition properties. The suite is build on top of a general purpose tensor library which facilitates shared-memory parallelisation and management of large amounts of data. It is interfaced to and distributed as part of the quantum chemistry package Q-Chem.

The `adcm` suite currently features ADC methods for the calculation of excitation energies up to third order in perturbation theory. This includes special variants like the SOS approximation for valence excited states and the CVS approximation to compute core excitations. The calculation of excited state properties and transition properties is also available at the level of second order perturbation theory. Oscillator strengths for transitions from the ground state and between excited states can be obtained, as well as the dipole moments of the excited states. Furthermore, two-photon absorption probabilities are available for the excited states without the necessity to evaluate the usual sum-over-states expression.

More features are constantly being added to the `adcm` suite. Among these ongoing developments are the full support of the RI approximation and the Choleski decomposition for the calculation of excitation energies [77]. Also excited state gradients for subsequent geometry optimisation on the excited state hypersurfaces are currently being implemented for all available ADC-variants and will soon be available. In addition, further properties and transition properties of the excited states are made available, like hyper-polarisabilities or spin-orbit couplings. Ultimately, we aim at a suite of excited state methods with the help of which it shall even be possible to perform ab initio molecular excited-state dynamics simulations.

5. Acknowledgements

MW gratefully acknowledges funding by the Alexander von Humboldt foundation in terms of a Feodor-Lynen fellowship. DRR, JW and CMK are supported by the Heidelberg Graduate School of Mathematical and Computational Methods for the Sciences.

References

- [1] L. Gonzalez, D. Escudero and L. Serrano-Andres, *Chem. Phys. Chem.* **13**, 28 (2012).
- [2] P.H.P. Harbach and A. Dreuw, in *Modeling of Molecular Properties*, edited by P. Comba (Wiley-VCH, Weinheim, 2011), p. 29.
- [3] A. Dreuw, *Chem. Phys. Chem.* **7**, 2259 (2006).
- [4] S. Grimme, *Rev. Comp. Chem.* **20**, 153 (2004).
- [5] M. Olivucci, editor, *Computational Photochemistry* (Elsevier Science B.V., Amsterdam, 2005).
- [6] M. Garavelli, *Theo. Chem. Acc.* **116**, 87 (2006).
- [7] W. Domcke, D.R. Yarkony and H. Köppel, editors, *Conical Intersections* (World Scientific Publishing, Singapore, 2004).

- [8] E. Runge and E.K.U. Gross, *Phys. Rev. Lett.* **52**, 997 (1984).
- [9] M.E. Casida, in *Recent Advances in Density Functional Methods, Part I*, edited by D. P. Chong (World Scientific, Singapore, 1995), pp. 155–192.
- [10] A. Dreuw and M. Head-Gordon, *Chem. Rev.* **105**, 4009 (2005).
- [11] P.J. Hay, *J. Phys. Chem. A* **106**, 1634 (2002).
- [12] M.K. Nazeeruddin, F. De Angelis, S. Fantacci, A. Selloni, G. Viscardi, P. Liska, S. Ito, B. Takeru and M. Grätzel, *J. Am. Chem. Soc.* **127**, 16835 (2005).
- [13] P.W. S. Suramitr, W. Meeto and S. Hannongbua, *Theo. Chem. Acc.* **125**, 35 (2010).
- [14] M. Wormit and A. Dreuw, *Phys. Chem. Chem. Phys.* **9**, 2917 (2007).
- [15] A. Dreuw, J.L. Weisman and M. Head-Gordon, *J. Chem. Phys.* **119**, 2943–2946 (2003).
- [16] D.J. Tozer, *J. Chem. Phys.* **119**, 12697 (2003).
- [17] J.H. Starcke, M. Wormit, J. Schirmer and A. Dreuw, *Chem. Phys.* **329**, 39 (2006).
- [18] T. Yanai, D.P. Tew and N.C. Handy, *Chem. Phys. Lett.* **393**, 51 (2004).
- [19] Y. Tawada, T. Tsuneda, S. Yanagisawa, T. Yanai and K. Hirao, *J. Chem. Phys.* **120**, 8425 (2004).
- [20] M.A. Rohrdanz, K.M. Martins and J.M. Herbert, *J. Chem. Phys.* **130**, 054112 (2009).
- [21] J.D. Chai and M. Head-Gordon, *Phys. Chem. Chem. Phys.* **10**, 6615 (2008).
- [22] O.A. Vydrov and G.E. Scuseria, *J. Chem. Phys.* **125** (23), 234109 (2006).
- [23] T. Stein, L. Kronik and R. Baer, *J. Am. Chem. Soc.* **131**, 2818 (2009).
- [24] J. Plötner, D.J. Tozer and A. Dreuw, *J. Chem. Theo. Comp.* **6**, 2351 (2010).
- [25] S. Grimme, *J. Chem. Phys.* **124**, 034108 (2006).
- [26] M.E. Casida, *J. Chem. Phys.* **122**, 054111 (2005).
- [27] R.G. Parr and W. Yang, *Density-Functional Theory of Atoms and Molecules* (Oxford Science Publication, New York, 1989).
- [28] D. Hegarthy and M.A. Robb, *Mol. Phys.* **38**, 1795 (1979).
- [29] R.H.E. Eade and M.A. Robb, *Chem. Phys. Lett.* **83**, 362 (1981).
- [30] H. Nakatsuji and K. Hirao, *J. Chem. Phys.* **68**, 2053 (1978).
- [31] O. Christiansen, H. Koch and P. Jørgensen, *J. Chem. Phys.* **103**, 7429 (1995).
- [32] H. Koch, O. Christiansen, P. Jørgensen, T. Helgaker and A.S. de Meras, *J. Chem. Phys.* **106**, 1808 (1997).
- [33] C. Haettig and F. Weigend, *J. Chem. Phys.* **113**, 5154 (2000).
- [34] C. Haettig, *Adv. Quant. Chem.* **50**, 37 (2005).
- [35] E.S. Nielsen, P. Jørgensen and J. Oddershede, *J. Chem. Phys.* **73**, 6238 (1980).
- [36] S.P.A. Sauer, *J. Phys. B: At. Mol. Opt. Phys.* **30**, 3773 (1997).
- [37] J.J. Eriksen, S. Sauer, K.V. Mikkelsen, H.J.A. Jensen and J. Kongsted, *J. Comp. Chem.* **33**, 2012 (2013).
- [38] J. Schirmer, *Phys. Rev. A* **26**, 2395 (1982).
- [39] A.B. Trofimov and J. Schirmer, *J. Phys. B* **28**, 2299 (1995).
- [40] J.H. Starcke, M. Wormit and A. Dreuw, *J. Chem. Phys.* **130**, 024104 (2009).
- [41] J. Schirmer, *Phys. Rev. A* **43**, 4647 (1991).
- [42] J. Schirmer and A.B. Trofimov, *J. Chem. Phys.* **120**, 11449 (2004).
- [43] A.B. Trofimov, G. Stelter and J. Schirmer, *J. Chem. Phys.* **111**, 9982 (1999).
- [44] P.R. Monson and W.M. McClain, *J. Chem. Phys.* **53**, 29 (1970).
- [45] P. Cronstrand, Y. Luo and H. Ågren, in *Response Theory and Molecular Properties (A Tribute to Jan Lindenberg and Poul Jørgensen)*, edited by H. J. A. Jensen, *Adv. Quant. Chem.*, Vol. 50 (, , 2005), pp. 1 – 21.
- [46] Y. Shao, L.F. Molnar, Y. Jung, J. Kussmann, C. Ochsenfeld, S.T. Brown, A.T.B. Gilbert, L.V. Slipchenko, S.V. Levchenko, D.P. O'Neill, R.A.D. Jr., R.C. Lochan, T. Wang, G.J.O. Beran, N.A. Besley, J.M. Herbert, C.Y. Lin, T.V. Voorhis, S.H. Chien, A. Sodt, R.P. Steele, V.A. Rassolov, P.E. Maslen, P.P. Korambath, R.D. Adamson, B. Austin, J. Baker, E.F.C. Byrd, H. Dachsel, R.J. Doerksen, A. Dreuw, B.D. Dunietz, A.D. Dutoi, T.R. Furlani, S.R. Gwaltney, A. Heyden, S. Hirata, C.P. Hsu, G. Kedziora, R.Z. Khalliulin, P. Klunzinger, A.M. Lee, M.S. Lee, W. Liang, I. Lotan, N. Nair, B. Peters, E.I. Proynov, P.A. Pieniazek, Y.M. Rhee, J. Ritchie, E. Rosta, C.D. Sherrill, A.C. Simmonett, J.E. Subotnik, H.L.W. III, W. Zhang, A.T. Bell and A.K. Chakraborty, *Advances in methods and algorithms in a modern quantum chemistry program package* *Phys. Chem. Chem. Phys.* **8**, 3172–3191 (2006).
- [47] A.I. Krylov and P.M. Gill, *WIREs Comput. Mol. Sci.* **3**, 317 (2013).
- [48] E. Epifanovsky, M. Wormit, T. Kuś, A. Landau, D. Zuev, K. Khistyayev, P. Manohar, I. Kaliman, A. Dreuw and A.I. Krylov, *J. Comp. Chem.* p. n/a (2013).
- [49] J. del Bene, R. Ditchfield and J.A. Pople, *J. Chem. Phys.* **55**, 2236 (1971).
- [50] O. Christiansen, H. Koch and P. Jørgensen, *Chem. Phys. Lett.* **243**, 409 (1995).
- [51] M. Head-Gordon, R.J. Rico, M. Oumi and T.J. Lee, *Chem. Phys. Lett.* **219**, 21 (1994).

- [52] M. Head-Gordon, A.M. Grana, D. Maurice and C.A. White, *J. Phys. Chem.* **99**, 14261 (1995).
- [53] H. Sekino and R.J. Bartlett, *Int. J. Quant. Chem. Symp.* **18**, 255 (1984).
- [54] J. Geertsen, M. Rittby and R.J. Bartlett, *Chem. Phys. Lett.* **164**, 57 (1989).
- [55] A.I. Krylov, *Ann. Rev. Phys. Chem.* **59**, 433 (2008).
- [56] E.R. Davidson, *J. Comp. Phys.* **17**, 87 (1975).
- [57] L.S. Cederbaum, W. Domcke and J. Schirmer, *Phys. Rev. A* **22**, 206 (1980).
- [58] O. Plekan, V. Feyer, R. Richter, M. Coreno, M. de Simone, K.C. Prince, A.B. Trofimov, E.V. Gromov, I.L. Zaytseva and J. Schirmer, *Chem. Phys.* **347**, 360 (2008).
- [59] A.B. Trofimov, T.E. Moskovskaya, E.V. Gromov, H. Köppel and J. Schirmer, *Phys. Rev. A* **64**, 022504 (2001).
- [60] A.B. Trofimov, T.E. Moskovskaya, E.V. Gromov, N.M. Vitkovskaya and J. Schirmer, *J. Struct. Chem.* **41**, 483 (2000).
- [61] T. Fransson, S. Coriani, O. Christiansen and P. Norman, *J. Chem. Phys.* **124311**, 138 (2013).
- [62] S. Grimme, *J. Chem. Phys.* **118**, 9095 (2003).
- [63] R.F. Fink, *J. Chem. Phys.* **133**, 174113 (2010).
- [64] S. Grimme, L. Goerigk and R.F. Fink, *WIREs Comput. Mol. Sci.* **2**, 886 (2012).
- [65] Y. Jung, R.C. Lochan, A.D. Dutoi and M. Head-Gordon, *J. Chem. Phys.* **121**, 9793 (2004).
- [66] S. Grimme and E. Izgorodina, *Chem. Phys.* **305**, 223 (2004).
- [67] Y.M. Rhee and M. Head-Gordon, *J. Phys. Chem. A* **113**, 10564 (2009).
- [68] M. Head-Gordon, M. Oumi and D. Maurice, *Mol. Phys.* **96**, 593 (1999).
- [69] D. Casanova, Y.M. Rhee and M. Head-Gordon, *J. Chem. Phys.* **128**, 164106 (2008).
- [70] Y.M. Rhee, D. Casanova and M. Head-Gordon, *J. Phys. Chem. A* **111**, 5314 (2007).
- [71] A. Hellweg, S.A. Grün and C. Hättig, *Phys. Chem. Chem. Phys.* **10**, 4119 (2008).
- [72] N.O. Winter and C. Hättig, *J. Chem. Phys.* **134**, 184101 (2011).
- [73] C.M. Krauter, M. Pernpointner and A. Dreuw, *J. Chem. Phys.* **138**, 044107 (2013).
- [74] TURBOMOLE V6.2 2010, a development of University of Karlsruhe and Forschungszentrum Karlsruhe GmbH, 1989-2007, TURBOMOLE GmbH, since 2007; available from <http://www.turbomole.com>.
- [75] M. Schreiber, M.R. Silva-Junior, S.P.A. Sauer and W. Thiel, *J. Chem. Phys.* **128**, 134110 (2008).
- [76] M. Head-Gordon, D. Maurice and M. Oumi, *Chem. Phys. Lett.* **246**, 114 (1995).
- [77] F. Aquilante, L. Boman, J. Boström, H. Koch, R. Lindh, A. Sánchez de Merás and T.B. Pedersen, *Challenges and Advances in Computational Chemistry and Physics* **13**, 301 (2011).
- [78] W. Humphrey, A. Dalke and K. Schulten, *J. Mol. Graph.* **14**, 33-38 (1996).

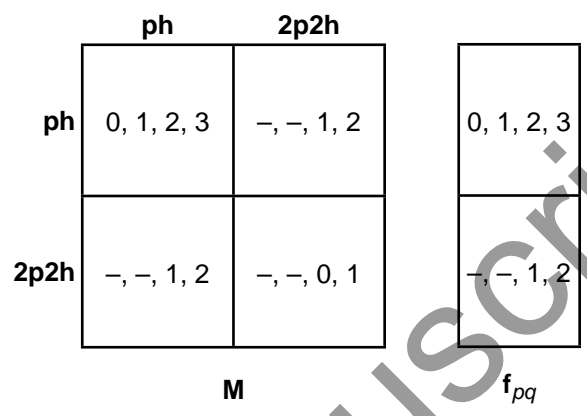


Figure 1. Structure of the ADC matrix M and spectroscopic amplitudes f_{pq} for up to third order in perturbation theory. In every block the order of the terms contributing to this block at a given overall order in perturbation theory is given. For example, in the ph/2p2h block of the ADC matrix there are no zeroth and first order terms contributing to this block. The earliest terms contributing to this block are first order terms which contribute at second order. At third order, additional second order terms are added.

Downloaded by [Aston University] at 16:44 20 January 2014

Accepted Manuscript

$$\begin{aligned}
 w_{ijab} = & \sum_c (v_{ijac}f_{bc} - f_{ac}v_{ijbc}) & w(i|j|a|b) = & \text{asymm}(a, b, \\
 & - \sum_k (f_{ik}v_{kjab} - f_{jk}v_{kiab}) & ! & \text{contract}(c, v_{\text{ooov}}(i|j|a|c), f_{\text{vv}}(b|c))) \\
 & - \frac{1}{2} \sum_k (\langle ij||ka \rangle v_{kb} - \langle ij||kb \rangle v_{ka}) & ! & - \text{asymm}(i, j, \\
 & + \frac{1}{2} \sum_c (v_{ic}\langle jc||ab \rangle - v_{jc}\langle ic||ab \rangle) & ! & \text{contract}(k, f_{\text{oo}}(i|k), v_{\text{ooov}}(k|j|a|b))) \\
 & & & - 0.5 * \text{asymm}(a, b, \\
 & & & ! \text{contract}(k, i_{\text{ooov}}(i|j|k|a), v_{\text{ov}}(k|b))) \\
 & & & + 0.5 * \text{asymm}(i, j, \\
 & & & ! \text{contract}(c, v_{\text{ov}}(i|c), i_{\text{ovvv}}(j|c|a|b)));
 \end{aligned}$$

Figure 2. Comparison of an ADC equation to its actual implementation using `libtensor`.

Accepted Manuscript

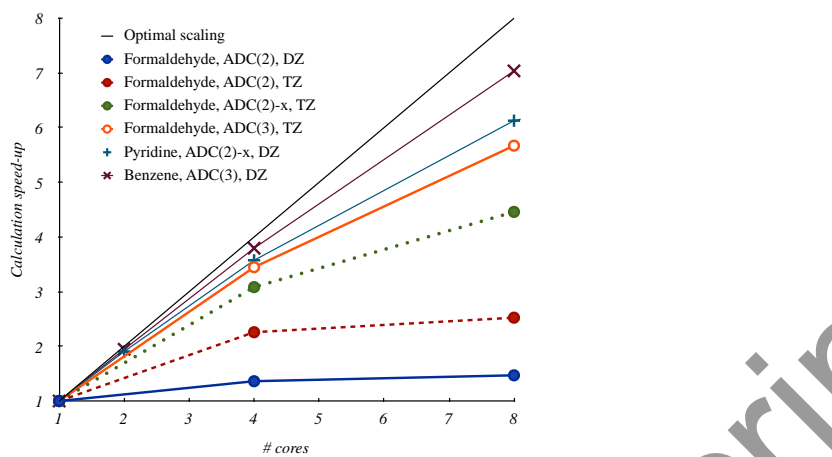


Figure 3. Scaling behaviour of the ADC implementation for up to 8 cores on Intel Xeon CPUs with up to 1 TB of memory. The calculations were performed keeping all data in memory. The abbreviations DZ and TZ refer to the aug-cc-pVDZ and aug-cc-pVTZ basis sets employed in the calculations.

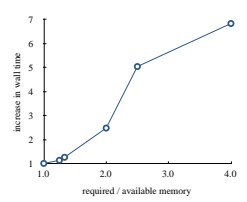


Figure 4. Increase in wall time due to limited memory for the ADC(2) calculation of benzene with aug-cc-pVDZ basis using the Davidson method. The required memory of the calculation is approx. 20 GB. The increase in wall time is given by $\frac{\text{actual wall time}}{\text{minimum wall time}}$ as function of $\frac{\text{required memory}}{\text{available memory}}$.

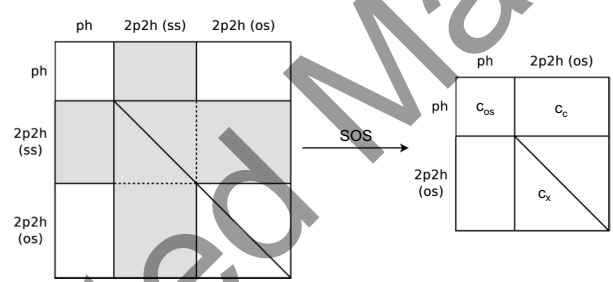


Figure 5. Schematic representation of the effect of the SOS approximation on the dimensionality of the ADC(2) matrix.

Downloaded by [Aston University] at 16:44 20 January 2014

Accepted Manuscript

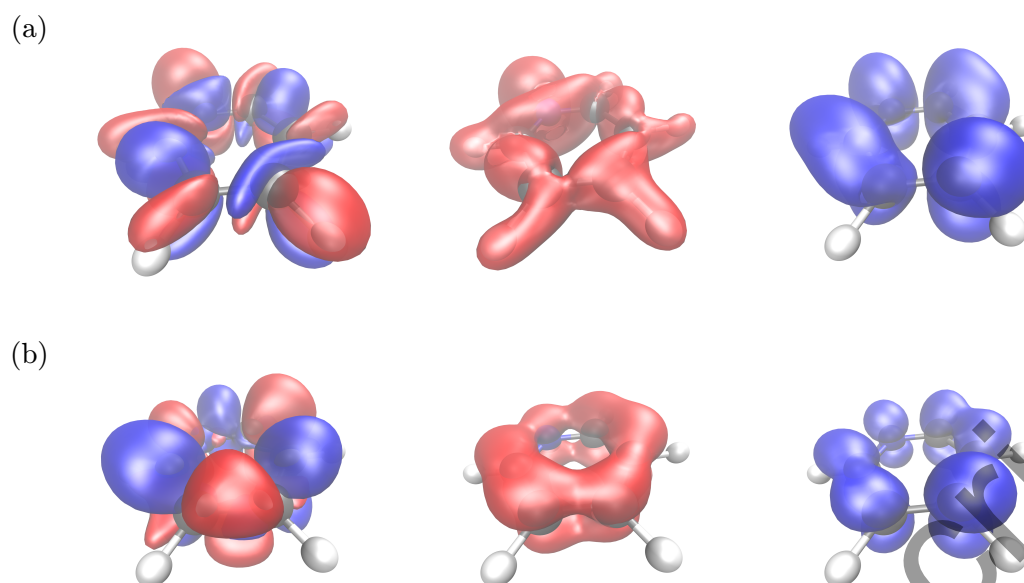


Figure 6. Transition densities (left) and attachment (middle) and detachment (right) densities of the two energetically lowest singlet excited states of pyridine calculated with ADC(3) and aug-cc-pVDZ basis set: (a) 1^1B_2 and (b) 1^1B_1 . The plots were obtained using the VMD program [78]. Positive parts of the transition densities and the attachment densities are displayed in red, while the negative parts of the transition densities and the detachment densities are displayed in blue.

Table 1. Excitation energies (in eV) of the two energetically lowest singlet excited states of formaldehyde computed using ADC(2), ADC(2)-x, and ADC(3) methods and three different basis sets. Oscillator strengths are given in parentheses below. In addition, the wall times (in minutes) for the calculations run on a Intel Xeon machine with 16 cores and 128GB memory are listed.

| Basis set | ADC(2) | | | ADC(2)-x | | | ADC(3) | | |
|-------------|-----------------|-----------------|------|-----------------|-----------------|------|-----------------|-----------------|-------|
| | 1^1A_2 | 1^1B_1 | Time | 1^1A_2 | 1^1B_1 | Time | 1^1A_2 | 1^1B_1 | Time |
| aug-cc-pVDZ | 3.83 (0.000) | 6.25 (0.018) | 0.4 | 3.03 (0.000) | 5.97 (0.016) | 1.1 | 3.88 (0.000) | 7.59 (0.021) | 2.7 |
| aug-cc-pVTZ | 3.83 (0.000) | 6.49 (0.018) | 1.8 | 3.02 (0.000) | 6.18 (0.016) | 8.7 | 3.82 (0.000) | 7.65 (0.021) | 27.8 |
| aug-cc-pVQZ | 3.84 (0.000) | 6.59 (0.018) | 6.8 | 3.04 (0.000) | 6.28 (0.016) | 68.6 | 3.82 (0.000) | 7.68 (0.021) | 236.6 |

Table 2. Comparison of the fifteen lowest core-excited states of thymine for 1s-excitation from C calculated using our implementation of CVS-ADC(2)-x with previously published data and experimental values [58].

| State | CVS-ADC(2)-x/6-311++G** ^a | | CVS-ADC(2)-x/6-31+G ^b | | Expt. ^b |
|-------|--------------------------------------|-----------|----------------------------------|-----------|--------------------|
| | ω_{ex} [eV] | f_{osc} | ω_{ex} [eV] | f_{osc} | ω_{ex} [eV] |
| 1 | 284.84 | 0.025 | 287.02 | 0.024 | 284.9 (A) |
| 2 | 286.36 | 0.049 | 288.54 | 0.045 | 285.9 (B) |
| 3 | 286.89 | 0.000 | 288.97 | 0.000 | |
| 4 | 287.11 | 0.004 | 289.05 | 0.004 | |
| 5 | 287.29 | 0.000 | 289.38 | 0.000 | |
| 6 | 287.95 | 0.015 | 290.06 | 0.015 | 287.3 (C) |
| 7 | 288.03 | 0.007 | 289.98 | 0.007 | |
| 8 | 288.07 | 0.002 | 290.23 | 0.002 | |
| 9 | 288.24 | 0.058 | 290.42 | 0.056 | 287.8 (D) |
| 10 | 288.34 | 0.000 | 290.46 | 0.000 | |
| 11 | 288.39 | 0.004 | 290.37 | 0.005 | |
| 12 | 288.45 | 0.013 | 290.40 | 0.013 | |
| 13 | 288.63 | 0.000 | 290.62 | 0.000 | |
| 14 | 288.88 | 0.009 | 290.95 | 0.009 | 288.4 (E) |
| 15 | 289.10 | 0.002 | 291.00 | 0.002 | |

^aour work, ^bdata and assignment according to Ref. [58]

Table 3. Transition properties for the four energetically lowest states of pyridine calculated with ADC(3) and aug-cc-pVDZ basis set. The excitation energies from the ground state are given in the last column, while the diagonal contains the state dipoles in Debye. The remaining values are the oscillator strengths of the respective transition.

| | GS | 1^1B_2 | 1^1B_1 | 1^1A_2 | 2^1A_1 | ω_{ex} [eV] |
|----------|-------|----------|----------|----------|----------|--------------------|
| GS | 1.925 | 0.00472 | 0.03513 | 0.00000 | 0.00966 | 0.00 |
| 1^1B_2 | | 0.765 | 0.00000 | 0.00053 | 0.00008 | 5.02 |
| 1^1B_1 | | | 1.910 | 0.00007 | 0.00014 | 5.05 |
| 1^1A_2 | | | | 1.022 | 0.00000 | 5.73 |
| 1^1A_1 | | | | | 2.381 | 6.42 |

Table 4. Comparison of two-photon transition strengths obtained via the sum-over-states expression (TPA-SOS) and via the intermediate state representation (TPA-ISR) for the four (six) energetically lowest states of formaldehyde (benzene) calculated using the ADC(2) method and aug-cc-pVDZ basis set. The sum-over-states expression has been evaluated using 16 and 32 states in case of formaldehyde and benzene, respectively.

| | State | ω_{ex} [eV] | f_{osc} | TPA _{SOS} [a.u.] | TPA _{ISR} [a.u.] |
|--------------|--------------------------------|--------------------|-----------|---------------------------|---------------------------|
| Formaldehyde | 1 ¹ A ₂ | 3.87 | 0.000 | 0.66 | 0.26 |
| | 1 ¹ B ₁ | 6.25 | 0.022 | 273.14 | 143.86 |
| | 2 ¹ A ₁ | 7.26 | 0.057 | 298.96 | 201.82 |
| | 2 ¹ B ₁ | 7.36 | 0.034 | 4.70 | 6.13 |
| Benzene | 1 ¹ B _{3u} | 5.19 | 0.000 | 0.00 | 0.00 |
| | 1 ¹ B _{3g} | 6.33 | 0.000 | 163.02 | 101.30 |
| | 1 ¹ B _{2g} | 6.33 | 0.000 | 164.56 | 101.30 |
| | 1 ¹ B _{2u} | 6.40 | 0.000 | 0.00 | 0.0 |
| | 1 ¹ B _{1u} | 6.86 | 0.071 | 0.00 | 0.0 |
| | 1 ¹ A _u | 6.92 | 0.000 | 0.00 | 0.0 |

Accepted Manuscript

Appendix A. Density and Transition Density Matrices in ADC

As described in section 2, the one-particle reduced (transition) density matrices can be computed from the excited state eigenvectors \mathbf{Y}_n of the ADC matrix in combination with the spectroscopic amplitude vector \mathbf{f}_{pq} or the matrix of IS transition densities \mathbf{B}_{pq} . This requires explicit equations for \mathbf{f}_{pq} and \mathbf{B}_{pq} which have to be derived using the ISR representation for specific orders in perturbation theory. Combining them with the excited state eigenvectors directly yields the equations to compute the transition density matrices. The equations for transition density matrices up to second order in perturbation theory are presented below.

In the following occupied (hole) indices are referred to as i, j, \dots , while virtual (particle) indices are named a, b, \dots . For notational convenience the following abbreviations are used. The Møller-Plesset (MP) T_2 amplitudes are denoted by $t_{ijab} = \frac{\langle ij||ab \rangle}{\epsilon_a + \epsilon_b - \epsilon_i - \epsilon_j}$, while $\rho_{0,pq}^{(2)}$ refers to the MP(2) correction to the ground state density matrix. The elements of the density matrix correction are given by

$$\begin{aligned}\rho_{0,ij}^{(2)} &= -\frac{1}{2} \sum_{kab} t_{ikab}^* t_{jkab} \\ \rho_{0,ia}^{(2)} &= -\frac{1}{2(\epsilon_a - \epsilon_i)} \left[\sum_{jbc} t_{ijbc} \langle ja||bc \rangle + \sum_{jkb} \langle jk||ib \rangle t_{jkab} \right] \\ \rho_{0,ab}^{(2)} &= \frac{1}{2} \sum_{ijc} t_{ijac}^* t_{ijbc}\end{aligned}$$

A.1. Transition Density Matrices from the Ground State

The equations for the transition density matrices from the ground state are obtained from the perturbation expansion of \mathbf{f}_{pq} . In zeroth and in first order this results in the following non-zero contributions to the density matrices

$$\rho_{ai}^{n\leftarrow 0} = Y_{n,ia}^* \quad (0\text{th order}) \quad (\text{A1})$$

$$\rho_{ia}^{n\leftarrow 0} = -\sum_{jb} t_{ijab}^* Y_{n,jb}^* \quad (1\text{st order}). \quad (\text{A2})$$

where $Y_{n,ia}^*$ denotes the ph part of the excited state eigenvector. In second order, there are non-zero contributions to all four parts of the density matrix

$$\begin{aligned}\rho_{ij}^{n\leftarrow 0} &= -\sum_a \rho_{0,ia}^{(2)} Y_{n,ja}^* - \sum_{kab} Y_{n,ikab}^* t_{jkab} \\ \rho_{ia}^{n\leftarrow 0} &= -\sum_{jb} Y_{n,jb}^* t_{ijab}^D \\ \rho_{ai}^{n\leftarrow 0} &= \frac{1}{2} \sum_{jb} t_{ijab} \sum_{kc} t_{jkb}^* Y_{n,kc}^* - \frac{1}{2} \sum_b \rho_{0,ab}^{(2)} Y_{n,ib}^* + \frac{1}{2} \sum_j \rho_{0,ij}^{(2)} Y_{n,ja}^* \\ \rho_{ab}^{n\leftarrow 0} &= \sum_i Y_{n,ia}^* \rho_{0,ib}^{(2)} + \sum_{ijc} Y_{n,ijac}^* t_{ijbc}^*\end{aligned} \quad (\text{A3})$$

Here, Y_{ia}^* and Y_{ijab}^* refer to the ph and $2p2h$ part of the excited state eigenvectors, while the newly introduced intermediate t_{ijab}^D is given by

$$t_{ijab}^D = \frac{X_{ijab} - X_{jiab} - X_{ijba} + X_{jiba}}{\epsilon_a + \epsilon_b - \epsilon_i - \epsilon_j}$$

with $X_{ijab} = \sum_{ck} t_{ikac}^* \langle kb || jc \rangle - \frac{1}{8} \sum_{cd} \langle ab || cd \rangle t_{ijcd}^* - \frac{1}{8} \sum_{kl} \langle kl || ij \rangle t_{klab}^*$ (A4)

A.2. State-to-State Transition Density Matrices

Similar to the equations for transition density matrices from the ground state, the state-to-state transition density matrices are derived from the perturbation expansion of \mathbf{B}_{pq} . Before presenting the equations it is useful to introduce a few more intermediates

$$\begin{aligned} P_{ij}^{m \leftarrow n} &= - \sum_a Y_{m,ja}^* Y_{n,ia}, & Q_{ij}^{m \leftarrow n} &= - \sum_{kab} Y_{m,jkab}^* Y_{n,ikab} \\ P_{ab}^{m \leftarrow n} &= \sum_i Y_{m,ia}^* Y_{n,ib}, & Q_{ab}^{m \leftarrow n} &= \sum_{ijc} Y_{m,ijac}^* Y_{n,ijbc} \\ P_{ia}^{m \leftarrow n} &= -2 \sum_i Y_{m,jb}^* Y_{n,ijab}, & P_{ai}^{m \leftarrow n} &= -2 \sum_i Y_{m,ijab}^* Y_{n,jb} \\ R_{n,ia} &= \sum_{jb} t_{ijab}^* Y_{n,jb}, & S_{n,ij} &= \sum_{kab} t_{ikab}^* Y_{n,jkab}, & S_{n,ab} &= \sum_{ijc} t_{ijac}^* Y_{n,ijbc} \end{aligned}$$

where $Y_{m,ia}^*$ and $Y_{m,ijab}^*$ refer to the ph and $2p2h$ parts of the left excited state eigenvector, while $Y_{n,ia}$ and $Y_{n,ijba}$ denote the ph and $2p2h$ parts of the right excited state eigenvector. With these intermediates the zeroth order contributions to the transition density matrices become

$$\begin{aligned} \rho_{ij}^{m \leftarrow n} &= P_{ij}^{m \leftarrow n} + Q_{ij}^{m \leftarrow n}, & \rho_{ab}^{m \leftarrow n} &= P_{ab}^{m \leftarrow n} + Q_{ab}^{m \leftarrow n} \\ \rho_{ia}^{m \leftarrow n} &= P_{ia}^{m \leftarrow n}, & \rho_{ai}^{m \leftarrow n} &= P_{ai}^{m \leftarrow n} \end{aligned} \quad (\text{A5})$$

while all first order contributions vanish. Instead one obtains a wealth of second order contributions to all parts of the density matrices

$$\begin{aligned} \rho_{ij}^{m \leftarrow n} &= \frac{1}{2} \sum_k \left[P_{ik}^{m \leftarrow n} \rho_{0,kJ}^{(2)} + \rho_{0,ik}^{(2)} P_{kj}^{m \leftarrow n} \right] - \sum_a R_{m,ia}^* R_{n,ja} \\ &\quad - \frac{1}{2} \sum_{cdk} t_{ikcd} \sum_l t_{jlcd}^* P_{lk}^{m \leftarrow n} + \sum_{cdk} t_{ikcd} \sum_b P_{cb}^{m \leftarrow n} t_{jkbd}^* \\ &\quad - \frac{1}{2} \sum_a Y_{n,ia} \sum_{ck} R_{m,kc}^* t_{jkac}^* - \frac{1}{2} \sum_a Y_{m,ja}^* \sum_{ck} t_{ikac} R_{n,kc} \end{aligned} \quad (\text{A6})$$

$$\begin{aligned}
\rho_{ab}^{m\leftarrow n} = & -\frac{1}{2} \sum_c \left[\rho_{0,ac}^{(2)} P_{cb}^{m\leftarrow n} + P_{ac}^{m\leftarrow n} \rho_{0,cb}^{(2)} \right] + \sum_i R_{m,ib}^* R_{n,ia} \\
& - \frac{1}{2} \sum_{ckl} t_{klbc} \sum_d t_{klad}^* P_{cd}^{m\leftarrow n} + \sum_{ckl} t_{klbc} \sum_j P_{jk}^{m\leftarrow n} t_{jlac}^* \\
& + \frac{1}{2} \sum_i Y_{n,ib} \sum_{ck} R_{m,kc}^* t_{ikac}^* + \frac{1}{2} \sum_i Y_{m,ia}^* \sum_{ck} t_{ikbc} R_{n,kc} \quad (\text{A7})
\end{aligned}$$

$$\begin{aligned}
\rho_{ia}^{m\leftarrow n} = & \sum_b P_{ba}^{m\leftarrow n} \rho_{bi}^{(2)} + \sum_j \rho_{aj}^{(2)} P_{ij}^{m\leftarrow n} - \sum_{bj} t_{ijab}^* P_{bj}^{m\leftarrow n} \\
& - \sum_c S_{m,ac}^* Y_{n,ic} - \sum_j S_{m,ij}^* Y_{n,ja} \quad (\text{A8})
\end{aligned}$$

$$\begin{aligned}
\rho_{ai}^{m\leftarrow n} = & \sum_b \rho_{ib}^{(2)} P_{ab}^{m\leftarrow n} + \sum_j P_{ji}^{m\leftarrow n} \rho_{ja}^{(2)} - \sum_{bj} t_{ijab} P_{jb}^{m\leftarrow n} \\
& - \sum_c Y_{m,ic}^* S_{n,ac} - \sum_j Y_{m,ja}^* S_{n,ij} \quad (\text{A9})
\end{aligned}$$

The equations above can also yield the excited state density matrices ρ_{pq}^n . Therefore, the same excited state eigenvector has to be employed as left and right vectors $\mathbf{Y}_m = \mathbf{Y}_n$. The resulting density matrices then represent the difference density matrix between the excited state and the ground state.